JOURNAL OF MATERIALS SCIENCE 31 (1996) 1345–1352

Dielectric and electrical properties of ordinary Portland cement and slag cement in the early hydration period

X. ZHANG, X.Z. DING, C.K. ONG, B.T.G. TAN
Department of Physics, National University of Singapore, Singapore 0511
J. YANG
Ssang Yong Cement (Singapore) Limited, 17 Pioneer Crescent, Singapore 2262

The dielectric constant and electrical conductivity of ordinary Portland cement (OPC) with water–cement ratios (w/c) of 0.30, 0.35 and 0.40 were measured for the first 30 h hydration, using a microwave technique in the frequency range 8.2–12.4 GHz. It was found that both the dielectric constant and electrical conductivity of the cement paste are sensitive to the water–cement ratio, the higher the w/c value, the greater the dielectric constant and electrical conductivity, and the longer the hydration time. We also found that the higher the frequency the greater the electrical conductivity but the smaller the dielectric constant. The dielectric constant and electrical conductivity of high- and low-slag cement with water–solid ratio (w/s) of 0.40 were measured in the first 30 h after mixing. The changes in dielectric constant and electrical conductivity of low-slag cement with time are similar to that of OPC, but the high-slag cement shows very different dielectric and electrical properties compared with OPC and low-slag cement. The relationship between the dielectric and electrical properties of cement paste and cement hydration was also discussed.

1. Introduction

Cement is a principal ingredient of construction materials such as concrete. Investigating the different mechanisms involved in cement hydration in plain cement paste and in concrete, especially in the early cement hydration period, is still a challenging problem because the early cement hydration involves very complicated chemical and physical processes. The principal techniques used to study this problem are X-ray diffraction, electron microscopy, thermal analysis and conduction calorimetry. X-ray diffraction is used for identifying hydration products in cement paste [1, 2]. Electron microscopy is used to monitor the development of microstructures in cement paste [3–5] and on the cement aggregate interface [6–8]. Thermal analysis [9, 10] is mainly useful for following the phase changes in relatively young cement paste. All these three methods are non-continuous methods and are not suitable for investigating the cement hydration *in situ*. Conduction calorimetry [11] is a continuous method, and it is most widely used for the study of cement hydration *in situ*. However, it only relates the processes which involve changes in heat, so it provides little information during the induction period of cement hydration, which only involves slight heat changes. Since the late 1970s, there has been increased interest in using electrical methods to study the early stage of cement hydration [12–28], because electrical methods are also continuous methods and can be used to study the cement hydration *in situ*.

Cement paste is the hydration product of unhydrated cement and water. During cement hydration the water molecule in cement paste changes from free water to water bound in various states of hydration or crystallization. This will change the ionic conduction of cement paste and will also affect the dielectric relaxation of cement paste. Moreover, as the water molecule changes from one bonding state to another, its ability to orient in an applied electric field changes. Thus the changes in the dielectric constant and electrical conductivity during hydration will reflect the changes of the bonding state of cement paste, and hence be related to the change of hydration products. The sensitivity of the dielectric constant and electrical conductivity to water content and the microstructure of cement paste suggests that the dielectric and electrical parameters could be used to monitor the hydration process in cement paste.

Most measurements of the dielectric and electrical parameters of cement paste have been performed using a parallel plate capacitor, i.e. the cement paste (as dielectric medium) is placed between two electrodes to form a capacitor. The change in capacitance of this "cement capacitor" is monitored during hydration. The dielectric constant and electrical conductivity (or resistivity) of cement paste are then obtained from the

0022–2461

capacitance measurement. It is reported [29] that using this method a simple conductance is in series with large lossy capacitance due to very thin dipole double layers formed at the electrodes. Although the dielectric constant of the interfacial layer at the electrodes may be small, the capacitance can be large due to the very small thickness of the layer. This unknown "electrode polarization" effect often causes difficulty in interpreting the conductance measurements. The problems can be minimized by substituting low-frequency a.c. measurements for d.c. measurements or by using four-probe techniques.

Another alternative is to use the microwave technique, as microwave measurements do not need electrodes and microwaves are sensitive to the water content. Reboul [30] has measured the complex dielectric constant of C_3S (Ca_3SiO_5) pastes by microwave measurements at 3 GHz for the first 30 h hydration. They have reported that the changes in dielectric behaviour lead to the discrimination of the reaction into three phases, which might correspond to three subsequent mechanisms. Wittman and Schlude [31] carried out measurements in the X-band (8.5–12.3 GHz). They found a monotonic decrease with time of both the real and imaginary parts of the dielectric constant. Using the transmission wave-guide technique, Gorur *et al.* [13] measured the changes in complex dielectric constant of cement paste with different water–cement ratios (w/c) in the first 48 h hydration at a frequency of 9 GHz. They related the changes in dielectric properties of hydrating cement to its free-water content. Moukwa *et al.* [26] measured the dielectric constant and electrical conductivity of three types of cement during the first 24 h hydration at 10 GHz using an infinite sample method. The correlation between the electrical parameters and the chemical processes were discussed. Although many works have been performed on ordinary Portland cement (OPC), the study of dielectric and electrical properties of slag cement is rare [22].

In this paper we report the results of the microwave measurement of the dielectric constant and electrical conductivity of ordinary Portland cement and slag cements during the first 30 h hydration.

2. Dielectric measurements and sample preparation

Investigations of the dielectric property of materials at microwave frequencies are typically conducted by filling a rectangular wave-guide section with a sample of the material and then determining the complex dielectric constant from measurements of the reflection and/or transmission coefficients of the dominant wave guide mode [32, 33]. The equipment used in this work consists of a microwave vector network analyser (HP8719C) with a coax-to-waveguide adapter (HP-X281C) and a sample holder consisting of a section of the standard WR-90 wave guide. An IBM-compatible personal computer (PC486) is set up to receive data over an IEEE-488 bus and to then perform subsequent numerical analysis. A materials measurement software is used for all necessary network analyser control, calculation, and data presentation. The software controls the network analyser in the measurement of the complex reflection coefficients S_{11} and S_{22}, and transmission coefficients S_{12} and S_{21} of the sample in the wave-guide sample holder. It then calculates the complex dielectric constant of cement paste using these four S parameters for the whole frequency range. The transmission wave-guide method is used for measuring the dielectric properties of cement paste in the frequency range 8.2–12.4 GHz. A schematic diagram of the experimental apparatus is shown in Fig. 1. The sample is placed into a wave guide which is connected between the two measurement planes, with one end of the sample hard against the PTFE plug. The insertion of a PTFE plug is to avoid leakage of water and cement paste from the sample holder as the wave-guide structure is set up vertically (this allow measurement of high water–cement ratio cement paste). We calibrated the measuring system at reference planes A and B so the effect of the PTFE plug is removed.

Ordinary portland cement (OPC) and low- and high-slag cements were used in this work. The compositions of these cements are given in Table I. Deionized water was used. The water–cement ratios (w/c) of 0.30, 0.35 and 0.40 were used for OPC and a water–solid ratio (w/s) of 0.40 was used for slag cements. The cement paste was carefully compacted into a rectangular wave guide with a size of

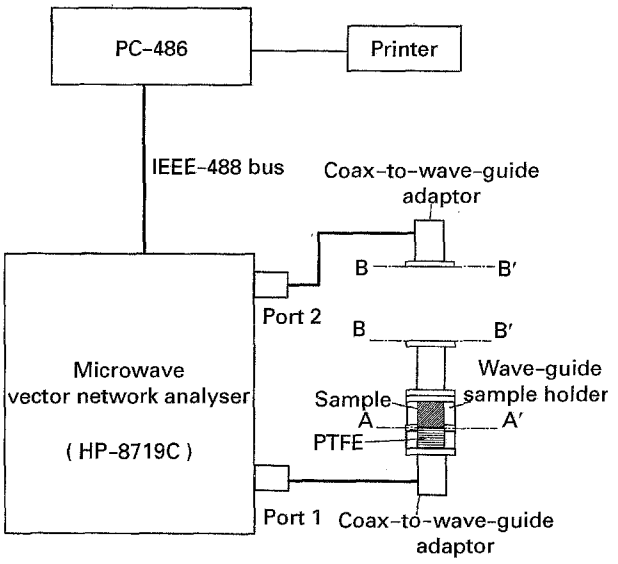

Figure 1 A schematic diagram of the experimental apparatus.

TABLE 1 Component oxides (wt %) in OPC and slag cements used

	Opc	Low-slag cement	High-slag cement
SiO_2	21.3	23.9	28.5
Al_2O_3	5.2	7.8	10.7
Fe_2O_3	2.8	2.3	1.8
CaO	62.6	56.8	48.6
MgO	1.8	2.8	5.7
SO_3	2.0	2.9	2.2
Na_2O	0.27	0.09	0.18
K_2O	0.53	1.18	0.48
Free CaO	1.60	1.19	0.51
Loss on ignition	1.6	1.4	0.1

$22.86 \times 10.16 \times 10\,mm^3$. The first measurement was made at about 5 min after mixing with water. Further measurements were made at intervals of 5–10 min during the first 5 h and then at intervals of 0.5–2 h over the next 25 h. All measurements were made at $23 \pm 2\,°C$.

3. Results

3.1. Hydration of OPC

Our measurement technique can give the complex dielectric constant directly. Its real part, ε', is a relative dielectric constant (in this paper we use the notation dielectric constant, ε, to represent the real part of relative dielectric constant, ε'). Its imaginary part, ε'', is related to electrical conductivity, σ, via the formula $\sigma = \varepsilon_0 \varepsilon'' \omega$, where ε_0 is the dielectric constant in vacuum and ω is angular frequency. Fig. 2 shows the changes in dielectric constant ε of OPC with a w/c of 0.40 corresponding to the different measuring frequencies. In the first hour, ε decreases rapidly and ε drops by about 2% of its initial values. In the period 1–4 h, ε continues to decrease but at a slow rate of $-0.2\,h^{-1}$. Then ε starts to decrease rapidly at about 4 h. In the period 6–18 h, ε decreases at the fastest rate of about $-0.6\,h^{-1}$. After 18–19 h mixing with water, the decrease of ε slows down and in the period 20–30 h, ε decreases almost linearly at a rate of about $-0.16\,h^{-1}$. The frequency effect on dielectric constant is also shown in Fig. 1. It is found that the shape of ε curves with different frequencies are similar, but the values of ε are dependent on the frequency. The higher the frequency, the smaller is the dielectric constant.

Fig. 3 shows the changes in electrical conductivity, σ, of OPC with a w/c of 0.40 corresponding to the different measuring frequencies. We found that in the first hour of hydration, σ changes in the opposite way to ε. σ increases with time in the first hour of hydration. At about 1 h it reaches its highest value and then starts to decrease. In the period 1–4 h, σ decreases at slower rate and this period is supposed to correspond to the induction period. Similar to the changes in dielectric constant, the electrical conductivity, σ, starts to decrease rapidly after 4 h mixing with water, and it decreases at the fastest rate in the period 6–18 h. At 18–19 h, the changes in σ slow down, and in the period 20–30 h the rate of decrease of σ is much smaller than that in the period 6–18 h. A very obvious frequency effect on the electrical conductivity was found. The higher the frequency, the greater was the electrical conductivity. The change in the electrical conductivity is very much dependent on the frequency. For example, in the period 6–18 h, the electrical conductivity measured at 12.0 GHz decreases much faster ($-0.24(\Omega m)^{-1}\,h^{-1}$) than that measured at 8.5 GHz ($-0.15(\Omega m)^{-1}\,h^{-1}$). But in the period 20–30 h this difference becomes smaller.

Figs. 4 and 5 show the changes in dielectric constant and electrical conductivity of OPC with different w/c values at 9.5 GHz. Both the dielectric constant and electrical conductivity are found to be sensitive to water–cement ratio. The higher the w/c value, the greater the dielectric constant and electrical conductivity. For example, the values of ε and σ of OPC with w/c = 0.35 are, respectively, about 8% and 11% greater than the values of ε and σ at w/c = 0.30. The values of ε and

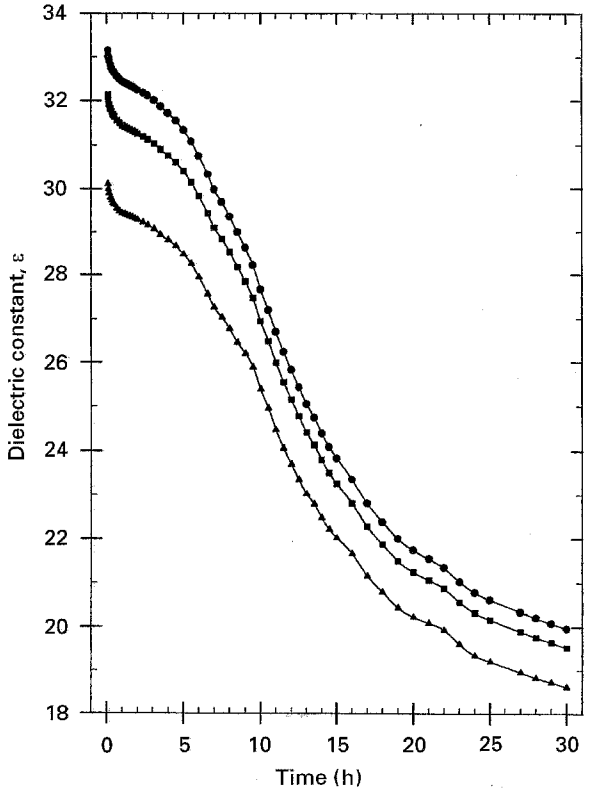

Figure 2 Variation of dielectric constant, ε, with time for OPC with w/c = 0.40 measured at frequencies of (●) 8.5, (■) 9.5 and (▲) 12.0 GHz.

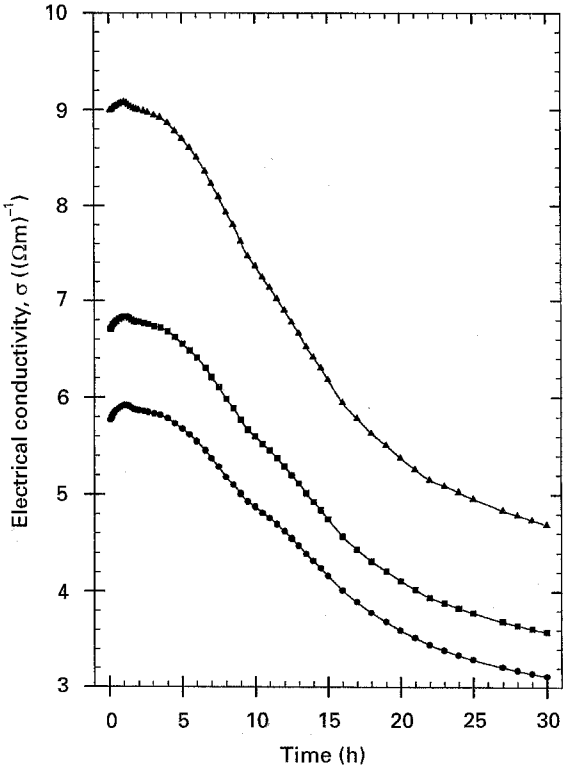

Figure 3 Variation of electrical conductivity, σ, with time for OPC with w/c = 0.40 measured at frequencies of (●) 8.5, (■) 9.5 and (▲) 12.0 GHz.

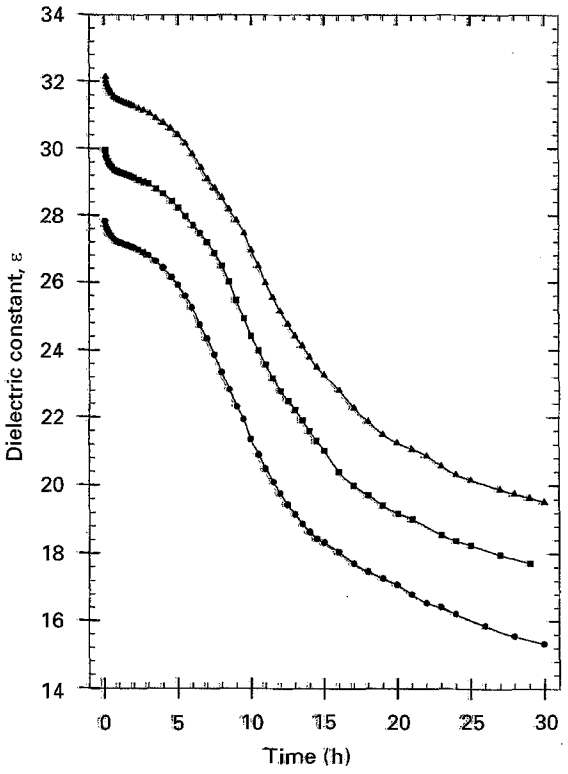

Figure 4 Variation of dielectric constant, ε, with time for OPC with w/c values of (●) 0.30, (■) 0.35 and (▲) 0.40 measured at a frequency of 9.5 GHz.

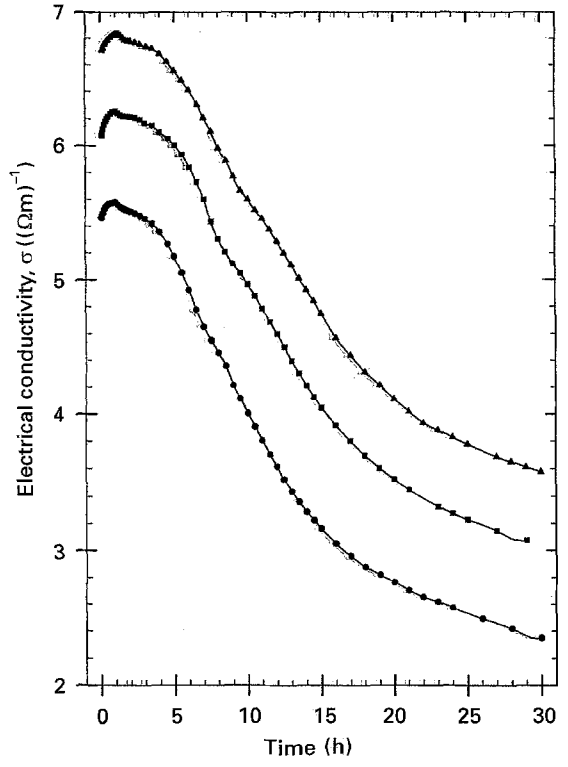

Figure 5 Variation of electrical conductivity, σ, with time for OPC with w/c values of (●) 0.30, (■) 0.35 and (▲) 0.40 measured at a frequency of 9.5 GHz.

σ at w/c = 0.40 are, respectively, about 7% and 10% greater than the values of ε and σ at w/c = 0.35. It is also found that with higher w/c values, the curves of dielectric constant and electrical conductivity shift to longer time. This is because the increase in water–cement ratio decelerates cement hydration. The induction period, which corresponds to the slow changes in the ε and σ curves in the period 1–3 h, is found to last longer as w/c increases. For all three w/c values, the induction period starts at about 1 h and ends at about 3, 3.5 and 4 h for respective w/c values of 0.30, 0.35 and 0.40. The last slow hydration period also starts later with increasing w/c values.

In order to see clearly the effect of w/c value on the dielectric constant, ε′, and electrical conductivity, σ, percentage changes in dielectric constant $\varepsilon(t)/\varepsilon(t_0)$ and percentage changes in electrical conductivity $\sigma(t)/\sigma(t_0)$ are shown in Figs 6 and 7, where $\varepsilon(t_0)$ and $\sigma(t_0)$ are the initial values of dielectric constant, ε, and electrical conductivity, σ, respectively, at time $t_0 = 5$ min. It is seen that after 7 h hydration, the OPC with higher w/c value will take a longer time to reach a particular $\varepsilon(t)/\varepsilon(t_0)$ or $\sigma(t)/\sigma(t_0)$ value compared

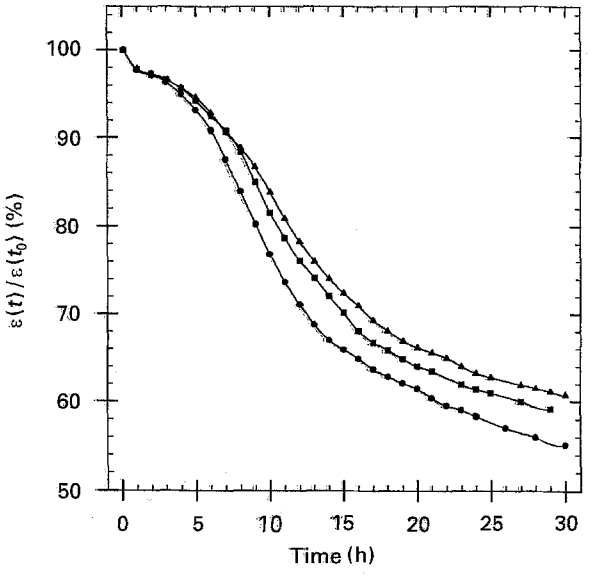

Figure 6 Variation of percentage changes in dielectric constant $\varepsilon(t)/\varepsilon(t_0)$ with time for OPC with w/c values of (●) 0.30, (■) 0.35 and (▲) 0.40 measured at a frequency of 9.5 GHz.

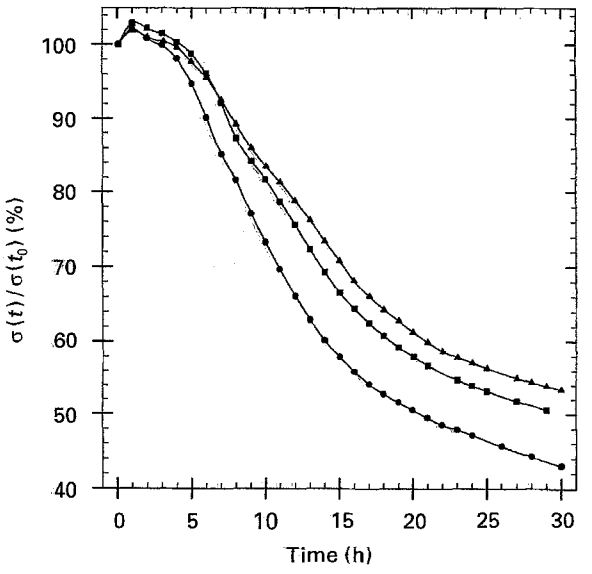

Figure 7 Variation of percentage changes in electrical conductivity $\sigma(t)/\sigma(t_0)$ with time for OPC with w/c values of (●) 0.30, (■) 0.35 and (▲) 0.40 measured at a frequency of 9.5 GHz.

with that with lower w/c value. This indicates that the higher the w/c value the slower is the cement hydration. It is also observed that the changes in electrical conductivity are faster than that of the dielectric constant, especially in the case of low w/c values. For example, at 15 h, ε of OPC with w/c = 0.30 drops by about 32% while σ drops by about 43%. We note that ε and σ curves have different shapes (see Figs 2–5) and their rates of change are also different (see Figs 6 and 7). These differences show that the measurement of dielectric constant and electrical conductivity may provide different information about cement hydration.

3.2. Hydration of slag cement

Fig. 8 shows the changes in dielectric constant, ε, of low-slag cement with time corresponding to different frequencies at a water–solid ratio (w/s) of 0.40. These curves are similar to those of OPC (see Figs 2 and 3) as their chemical compositions are not very different. There are some differences in the ε curves compared with those of OPC. The initial ε value of low-slag cement is less than that of OPC. In the first 20 min, the ε drops rapidly while for OPC this rapid drop period will last about 1 h. After 20 min mixing, ε drops linearly at a slow rate of $-0.26\ h^{-1}$ until about 5 h. Then ε decreases quickly at a rate of about $-0.7\ h^{-1}$ until about 16 h. At 16 h the changes in dielectric constant, ε, start to slow down. The frequency effect is also investigated. We find that the higher the frequency, the smaller are the ε values. We also note that the changes in ε at higher frequency are less than those at lower frequency.

The changes in electrical conductivity, σ, of low-slag cement with time corresponding to different frequencies at a water–solid ratio (w/s) of 0.40 is shown in Fig. 9, which are quite different from that of OPC at w/c = 0.40 (see Fig. 3). σ drops in the first 20 min and then increases until it reaches a peak at about 3–3.5 h. After 5 h mixing, σ decreases rapidly up to 10 h, and then it decreases slowly. The frequency effect on σ is the opposite to that for ε, i.e. the higher the frequency the higher is the σ value, and the changes in σ at higher frequency are greater than those at lower frequency.

Fig. 10 shows the changes in ε of high-slag cement with time at w/s = 0.40. It is observed that the changes in ε of high-slag cement are different from those of OPC. ε drops 3% in the first hour and then decreases slowly at the rate of $-0.1\ h^{-1}$ in the period 1–5 h. After 5 h mixing with water, ε decreases rapidly up to about 11 h but its rate of decrease is less than that of low-slag cement. In the period 11–30 h, ε decreases almost linearly at the rate of $-0.33\ h^{-1}$, which is faster than that of low-slag cement in the period 20–30 h. There is a small bump in the ε curves in the period 8–10 h which is not observed in OPC. The bump may be an indication of the reaction of slag because slag reacts much more slowly compared with OPC.

Fig. 11 shows the changes in σ of high-slag cement with time at w/s = 0.40. Again we observe that changes in σ in high-slag cement are different from those of OPC. σ drops first then it increases slowly until it reaches a peak at about 3–4 h. After this time, σ decreases at a slow rate upto 7 h, then it starts to drop rapidly. At 10 h, σ is found to increase slightly, which may correspond to the reaction of slag. This

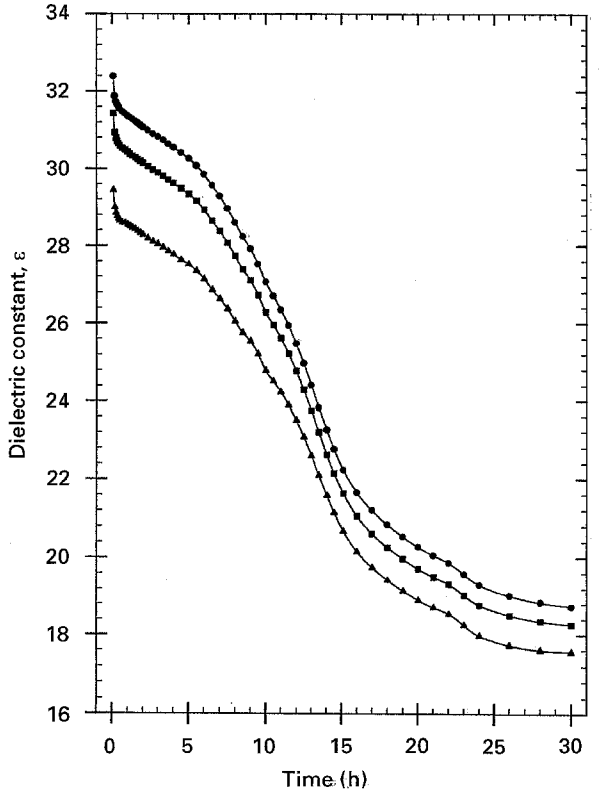

Figure 8 Variation of dielectric constant, ε, with time for low-slag cement with w/s = 0.40 measured at frequencies of (●) 8.5, (■) 9.5 and (▲) 12.0 GHz.

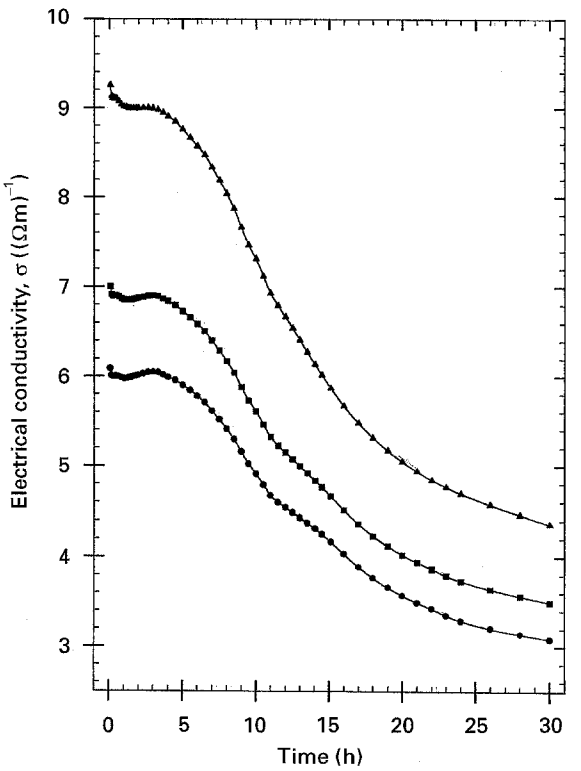

Figure 9 Variation of electrical conductivity, σ, with time for low-slag cement with w/s = 0.40 measured at frequencies of (●) 8.5, (■) 9.5 and (▲) 12.0 GHz.

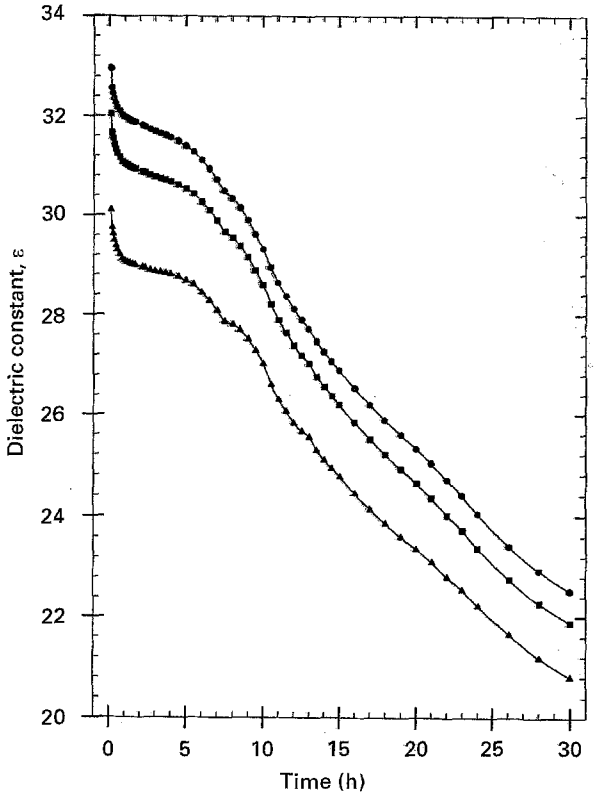

Figure 10 Variation of dielectric constant, ε, with time for high-slag cement with w/s = 0.40 measured at frequencies of (●) 8.5, (■) 9.5 and (▲) 12.0 GHz.

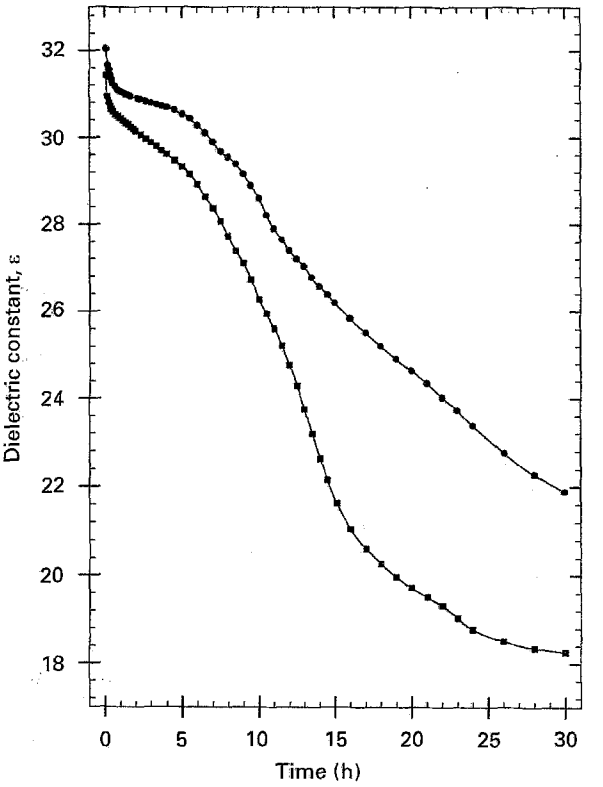

Figure 12 Comparison of dielectric constant, ε, between (■) low- and (●) high-slag cement with w/s = 0.40 measured at a frequency of 9.5 GHz.

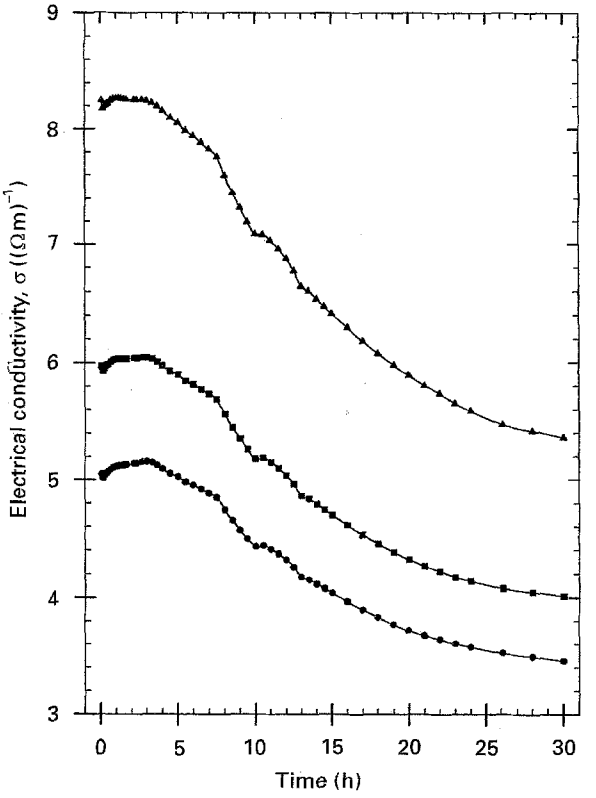

Figure 11 Variation of electrical conductivity, σ, with time for high slag cement with w/s = 0.40 measured at frequencies of (●) 8.5, (■) 9.5 and (▲) 12.0 GHz.

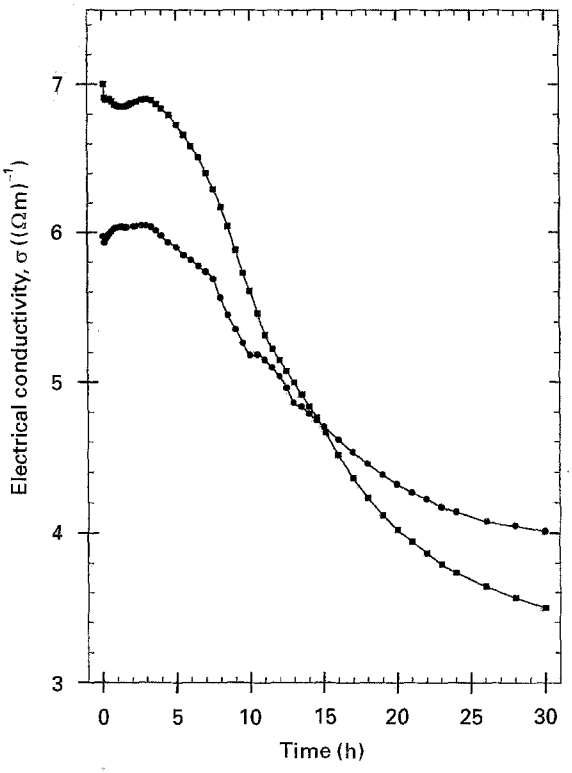

Figure 13 Comparison of electrical conductivity, σ, between (■) low- and (●) high-slag cement with w/s = 0.40 measured at a frequency of 9.5 GHz.

small increment results in a hump in the σ curves in the period 10–13 h. After 13 h mixing with water, σ decreases at a slower rate compared with that of low-slag cement. The frequency effect of high-slag cement is similar to that of low-slag cement, i.e. the higher the frequency, the higher is the σ value but lower the ε value.

A comparison of high-slag and low-slag was made (see Figs 12 and 13). The ε and σ curves of low-slag cement are more like those of OPC (see Figs 2 and 3)

but are different in the first 5 h. The high-slag cement shows large differences from low-slag cement. The ε values of high-slag cement are smaller than that of low-slag cement, and the σ values are smaller in the first 15 h and greater in the period 15–30 h than those of low-slag cement. Note that like low-slag cement and OPC, there is no rapidly dropping portion in the ε and σ curves for high-slag cement in the period 5–15 h. But small humps are observed in both ε and σ curves in the same period. It seems that there is no significant continuous change in ε and σ curves for high-slag cement, which may attribute to the slow reaction of slag.

4. Discussion

A number of factors in cement hydration will affect the dielectric constant and electrical conductivity of the cement paste. Examples of such factors are the changes in the physical state of water and ionic concentrations within the water, the ease with which dipoles and polar molecules can move within the cement paste, the degree of association of charges with the cement grain surface, and the temperature of the cement system. All these factors change with differences in the cement hydration process and hence the dielectric constant and electrical conductivity change with the cement hydration process. When OPC is mixed with water, a series of chemical reactions takes place. The reactions of cement with water proceed at different rates for the various mineral phases and involve both hydrolysis and hydration processes. The chemical processes of cement hydration can be categorized into four stages [34, 35].

1. Stage I. This stage is the first cement hydration period and it will last for about 15 min hydration. When water comes into contact with cement, the ions (primary Ca^{2+} and OH^-) rapidly leach from tricalcium silicate, C_3S (Ca_3SiO_5), and tricalcium aluminate, C_3A ($Ca_3Al_2O_6$), grain surface (they are two of the main components of cement). This causes the increase in ion concentration. In stage I, most ions are unbound charges in the aqueous phase. These unbound charges polarize and move easily in the electrical field, resulting in a large dielectric constant and a large electrical conductivity. Thus, in this stage, the dielectric constant and electrical conductivity of cement paste have large values as shown in Figs 2 and 3.

2. Stage II. Ions (primarily Ca^{2+} and OH^-) are rapidly leached from the cement grain surfaces leaving behind a surface layer rich in hydrosilicate ions on the C_3S and C_3A phase, giving the cement grain a net negative charge. Within a few minutes, an amorphous, semi-permeable gel membrane of calcium silicate hydrate, C–S–H, forms outside the surface layer. This surface layer, together with the grain and C–S–H, form an electrical double layer, resulting in a physical barrier separating the silica-rich surface layer and the diffuse electrical double layer. It is this electrical double layer which hinders the rapid dissolution of unhydrated cement grains, leading to the slow hydration rate in stage II. Thus, stage II is called the induction period, and it will last from 1–3 h depending on cement composition and w/c value.

During the induction period, Si^{4+} ion concentration decreases; Ca^{2+} ion concentration increases and reaches a supersaturation level. Early hydration products, calcium hydroxide, CH ($Ca(OH)_2$), and C–S–H nuclei, begin to form. The formation of these early hydration products causes the continuous increase in viscosity of the cement paste. This results in the difficulty of polarization and movement of the charged ions, leading to a decrease in the dielectric constant and electrical conductivity of cement paste. It has been reported that in this stage the dielectric constant and electrical conductivity decrease at a slow rate. Our results (see Figs 2 and 3) are also in agreement with these results.

3. Stage III. The rupturing of the electrical double layer allows water to reach the cement grains, leading to accelerated dissolution of the grain. This stage starts at about 3–4 h and ends at about 15–17 h after mixing with water (the time is dependent on the composition of the cement and the w/c value). While Ca^{2+} ions are removed from solution, hydration products C–S–H and CH are rapidly formed in this stage. As the hydration products build up on the cement grains and the C–S–H extends to form a fibrous rigid structure, the cement paste begins to stiffen (initial setting) and its porosity increases. The polar molecules and ions in the cement paste locked in the pores have difficultly contributing to the polarization, because polar molecules and ions become irrotationally bound, hence decreasing the polarizability of the cement paste. Rapid formation of the C–S–H and increase in porosity also cause the ions in the free water to have to follow a more tortuous path to drift through the pores, resulting in a decrease of electrical conductivity. The formation of hydration products proceeds at an accelerated rate, resulting in a sharp decrease in dielectric constant and electrical conductivity, as shown in Figs 2 and 3.

4. Stage IV. This is the last stage and it starts at about 15–17 h after mixing with water, and it can last for about 1 year. During this stage, the slow diffusion-controlled formation of C–S–H and CH takes place. Recrystallization of ettringite to monosulphate (they are also cement hydration products) and some polymerization of silicates are possible. In this period, the heat evolution and porosity decrease. Formation of particle-to-particle and paste-to-aggregate bonds takes place. Corresponding to the slow changes in the cement paste the dielectric constant and electrical conductivity continuously decrease but at a slow rate compared to that in stage III.

Compared with the hydration of OPC, slag cement has a slow hydration process. For low-slag cement, the ε and σ curves are more or less similar to that of OPC as their composition is not very different. But for high-slag cements (which have about 55% slag) the composition is very different from that of OPC, therefore the ε and σ curves are also very different from that of OPC, as expected. Compared with OPC, the main features of the ε and σ curves of high-slag cement are

the slow changes in ε and σ curves, because slag is not as reactive as OPC cement. As far as we are aware, the only conductivity measurement of slag cement was reported by Perez-Pena *et al.* [22]. They measured the electrical conductivity of MC500 slag cement. It was reported that σ increases slightly in the first 2 h and then a relatively sharper decrease in σ occurs in the period 2–4 h. Compared with MC500 slag cement, σ of our slag cements shows a slow decrease. This difference could be attributed to the relatively higher surface area of MC500 slag cement (8000 cm^2g^{-1} for MC500 against 3400 cm^2g^{-1} for our slag cements), as the hydration of slag cement is distinctly enhanced by an increase in the fineness of the slag cement [36]. In the σ curve of MC500 slag cement, a very small peak was observed about 5 h after mixing. We also observed a small peak in the σ curve at about 10 h after mixing. The time difference may be attributed to the slow hydration in our slag cement as MC500 slag cement is much finer than ours.

As our microwave techniques do not require the use of electrodes, the unknown "electrode polarization" caused by the electrodes is avoided. This makes our measurement more reliable and more accurate. The main measurement error in our experiment comes from the control of the thickness of the sample, as cement paste shrinks when it dries. We estimate our measurement error to be less than 5%. As for the high accuracy of our experimental method and sensitiveness of the microwave to water, our measuring system can easily distinguish a w/c difference of less than 0.025, as shown in Figs 4 and 5. It appears that our microwave technique can be used as a quick and reliable method to determine the w/c value in cement paste.

5. Conclusion

We have measured the dielectric constant and electrical conductivity of OPC with w/c values of 0.30, 0.35, and 0.40 in the frequency range 8.2–12.4 GHz in the first 30 h hydration. We found that both dielectric constant and electrical conductivity are sensitive to the water–cement ratio (w/c). The higher the w/c value, the greater were the values of dielectric constant and electrical conductivity, and the longer was the hydration time. The frequency effect on dielectric constant and electrical conductivity was also studied. We found that the higher the frequency, the greater was the electrical conductivity but the smaller was the dielectric constant. We also found that the responses of the dielectric constant and electrical conductivity of OPC to cement hydration are similar, but not the same, indicating that they may provide different information about cement hydration.

We have also measured the dielectric constant and electrical conductivity of low- and high-slag cements with a water-solid value of 0.40 in the frequency range 8.2–12.4 GHz in the first 30 h. It was found that the changes in ε and σ curves of low-slag cement are similar to that of OPC. But for high-slag cement, the ε and σ curves have very different shapes compared with those of OPC and low-slag cement.

We found that our microwave technique is sensitive enough to detect a w/c difference of less than 0.025. It appears that the microwave technique can be used as a quick and reliable method to determine the w/c value in cement paste.

References

1. P. L. PRATT, *Mater. Struct.* **21** (1988) 106.
2. K. MATHER, in "Evaluation of Methods of Identifying Phases of Cement Paste", edited by W. L. Dolch, Transportation Research Circular 176 (Transportation Research Board, Washington, 1976) p. 9.
3. D. MENETRIER, I. JAWED, T. S. SUN and J. SKAINY, *Cem. Concr. Res.* **9** (1979) 473.
4. K. L. SCRIVENER, in "Materials Science of Concrete I", edited by J. P. Skany (American Ceramic Society, Westerville, OH, 1989) p. 127.
5. G. W. GROVES, *J. Mater. Sci.* **16** (1981) 1063.
6. X. ZHANG and G. W. GROVES, *Mater. Sci. Technol.* **5** (1989) 714.
7. *Idem. Adv. Cem. Res.* **3** (1990) 15.
8. G. W. GROVES and X. ZHANG, *Cem. Concr. Res.* **20** (1990) 453.
9. L. BEN-DOR and D. PEREZ, *Thermochim. Acta* **12** (1975) 81.
10. J. BENSTED and S. P. VARMA, *Cem. Technol.* **5** (1974) 440.
11. H. F. W. TAYLOR, "*Cement Chemistry*", (Academic Press, London, 1990).
12. F. D. TAMAS, *Cem. Concr. Res.* **12** (1982) 115.
13. K. GORUR, M. K. SMIT and F. H. WITTMANN, *ibid.* **12** (1982) 447.
14. W. J. McCARTER and P. N. CURRAN, *Mag. Concr. Res.* **36** (1984) 42.
15. W. J. McCARTER and A. B. AFSHAR, *J. Mater. Sci. Lett.* **3** (1984) 1083.
16. *Idem, Proc. Inst. Civ. Eng. 2* **79** (1985) 585.
17. F. D. TAMAS, E. FARKAS, M. VOROS and D. M. ROY, *Cem. Concr. Res.* **17** (1987) 340.
18. W. J. McCARTER, *ibid.* **17** (1987) 55.
19. H. C. KIM and S. S. YOON, *J. Phys. D* **21** (1988) 1215.
20. W. J. McCARTER and A. B. AFSHAR, *J. Mater. Sci.* **23** (1988) 488.
21. W. J. McCARTER and S. GARVIN, *J. Phys. D.* **22** (1989) 1773.
22. M. PEREZ-PENA, D. M. ROY and F. D. TAMAS, *J. Mater. Res.* **4** (1989) 215.
23. M. A. BARI, *J. Phys. D* **23** (1990) 234.
24. J. G. WILSON and H. W. WHITTINGTON, *IEE Proc.* **137** Pt. A (1990) 246.
25. C. A. SCUDERI, T. O. MASON and H. M. JENNINGS, *J. Mater. Sci.* **26** (1991) 349.
26. M. MOUKWA, M. BRODWIN, S. CHRISTO, J. CHANG and S. P. SHAH, *Cem. Concr. Res.* **21** (1991) 863.
27. A. M. DUNSTER and J. R. PARSONAGE, *Chem. Ind.* (1992) Issue 8 304.
28. A. BERG, G. A. NIKLASSON, K. BRANTERVIK, B. HEDBERG and L. O. NILSSON, *J. Appl. Phys.* **71** (1992) 5897.
29. P. R. CAMP and S. BILOTTA, *J. Appl. Phys.* **66** (1989) 6007.
30. J. P. REBOUL, *Rev. Phys. Appl.* **13** (1978) 383.
31. F. W. WITTMANN and F. SCHLUDE, *Cem. Concr. Res.* **5** (1975) 63.
32. K. H. OH, C. K. ONG and B. T. G. TAN, *J. Phys. E Sci. Instrum.* **22** (1989) 876
33. X. Z. DING, LU TAIJING, C. K. ONG and B. T. G. TAN, *J. Appl. Phys.* **75** (1994) 7411.
34. I. JAWED, J. SKALNY and J. F. YOUNG, in "Structure and performance of cements", edited by P. Barnes, (Elsevier Science, London, 1983) p. 237.
35. S. MINDESS and J. F. YOUNG, "Concrete" (Prentice-Hall, 1981) pp. 76–7.
36. W. HINRICHS and I. ODLER, *Adv. Cem. Res.* **2** (1989) 9.

Received 9 August 1994
and accepted 8 September 1995